Interlayer interference in double wells in a tilted magnetic field

G. M. Gusev, C. A. Duarte, and T. E. Lamas

Instituto de Física da Universidade de São Paulo, CP 66318 CEP 05315-970, São Paulo, SP, Brazil

A. K. Bakarov

Institute of Semiconductor Physics, Novosibirsk 630090, Russia

J. C. Portal

GHMFL-CNRS, BP-166, F-38042, Grenoble, Cedex 9, France, INSA-Toulouse, 31077, Cedex 4, France
and Institut Universitaire de France, Toulouse, France

Magnetotransport measurements on bilayer electron systems reveal repeated reentrance of the resistance minima at filling factors $\nu=4N+1$ and $\nu=4N+3$, where N is the Landau index number, in the tilted magnetic field. At high filling factors, the Shubnikov-de Haas oscillations exhibit beating effects at certain tilt angles. We attribute such behavior to oscillations of the tunneling gap due to Aharonov-Bohm interference effect between cyclotron orbits in different layers. The interplay between quantum and quasiclassical regimes is established.

I. INTRODUCTION

Magnetoresistance of the normal-metal ring shows periodical oscillations as a function of the enclosed magnetic flux. This phenomenon, known as the Aharonov-Bohm (AB) effect, results from the interference between partial electronic waves encircling the conductor in opposite directions.[1] The AB effect has been observed in lithographically defined diffusive metallic and semiconductor rings,[2,3] ballistic semiconductor rings,[4,5] carbon nanotubes,[6] and self-assembled quantum rings.[7]

Recently oscillatory phenomena in quasi-one-dimensional organic semiconductor[8] and semiconductor bilayers[9] have been analyzed and interpreted as the AB effect, both in the real and momentum spaces.

The double quantum wells (DQWs), which consist of two quantum wells separated by a tunneling barrier, should be recognized as the most convenient system for studying the interlayer interference phenomenon, owing to high mobility. The quantum tunneling induces hybridization of the subband energies and introduces symmetric–antisymmetric energy Δ_{SAS} with the typical value of 0.1–1 meV. Recently it has been predicted that in high Landau levels the tunneling amplitude oscillates with the in-plane magnetic field,[10] which also has been confirmed in experiments.[11] Furthermore, it has been demonstrated that the so-called angular magnetoresistance oscillations (AMROs) discovered in quasi-two-dimensional organic conductors can be explained by the interference of the gauge phase difference between the layers.[12] However, the calculations[10] and experiments[11] have been focused on the low Landau-level (LL) indexes; therefore the relation of this effect to Aharonov-Bohm interference effect and AMRO was not recognized. It is worth noting that AMRO in organic conductors has been studied for high filling factors, and the relationship between semiconductor bilayers and other layered materials was demonstrated only recently in a theoretical paper.[9]

Due to a high mobility, the double quantum wells allow the studying of AMRO in both regimes: for small filling factors, when the quantum Hall effect is well resolved, and for high filling factors, when quasiclassical approximation is valid.

Here we present the magnetoresistance data acquired in the tilted magnetic field in double quantum wells with different barriers focusing on transport parallel to the layers. We found strong magnetoresistance oscillations as a function of the in-plane magnetic field at $\nu=4N+3$ and $\nu=4N+1$ filling factors. At low perpendicular magnetic field, the amplitude of the conventional Shubnikov-de Haas (SdH) oscillations also exhibits $B_\parallel$-periodic dependence at fixed values of $B_\perp$. We interpret the observed oscillations as a manifestation of the interference between cyclotron orbits in different quantum wells. The peak/value ratio exceeds 10^4–10^5.

II. EXPERIMENTAL RESULTS

The samples are symmetrically doped GaAs double quantum wells with equal widths $d_W=140$ Å separated by $Al_xGa_{x-1}As$ barriers with different width d_b varied from 14 to 31 Å. The samples have high total sheet electron density $n_s \approx 9 \times 10^{11}$ cm^{-2} (4.5×10^{11} cm^{-2} per one layer). Both layers are shunted by Ohmic contacts. The relative densities in the wells are varied by the top gate composed of a gold film. The voltage of the top gate raises or lowers only the density of the well which is closest to the sample surface (upper well) with carrier density in the bottom well being almost constant. The system is balanced at zero gate voltage. The balance point is determined from the measurements of the symmetric–antisymmetric gap as a function of the gate voltage. The value of this gap should have a minimum value at a resonance point. The energy of the symmetric–antisymmetric gap is extracted from the low-field double periodic Shubnikov-de Haas oscillations and magnetointersubband oscillations induced by resonance transitions between the tunneling-coupled states, which recently have been observed and explained in Ref. 13. Note that we did not see the resonance magnetoresistance at the balance point,[14] which

TABLE I. The sample parameters for balanced point at zero top gate voltage. d_W is the well width, d_b is the barrier thickness, $d = d_W + d_b$, d_{exp} is the distance between maxima of the wave functions, determined from AMRO periodicity, n_s is the electron density, and μ is the zero-field mobility. Δ_{SAS}^{theor} is the symmetric–antisymmetric splitting energy determined from self-consistent calculations.

d_b (Å)	d_W (Å)	d (Å)	d_{exp} (Å)	n_s (10^{11} cm^{-2})	μ (10^3 cm^2/Vs)	Δ_{SAS}^{theor} (meV)
14	140	154	115	9.32	970	3.87
20	140	160	125	9.2	900	2.59
31	140	171	125	9.19	870	1.24

may indicate that the mobility in two quantum wells is the same. Very likely it results from a symmetric structure of the sample and high electron density. At the resonance point, we observe no positive classical magnetoresistance, which also supports the fact that the mobility in the upper well is equal to the mobility in the lower well. Indeed, away from the resonance point, the two-subband positive magnetoresistance[15] is clearly seen.[13]

The symmetric–antisymmetric gap is also calculated from a self-consistent solution of the double-well Schrodinger equation and Poisson's equation. It is in reasonable agreement with the value extracted from the low-field double periodic Shubnikov-de Haas and magnetointersubband oscillations. The parameters of the samples are shown in Table I. Over a dozen specimens of both the Hall bars and van der Pauw geometries from three wafers have been studied. The Hall bars have rectangular dimensions of $500 \times 200 ~\mu$m^2. We measure both longitudinal and Hall resistances at the temperatures $T = 50$ mK for different tilt angles Θ between the normal to quantum well plane, and magnetic fields B up to 15 T using conventional ac-locking techniques with a bias current of $0.01-0.1 ~\mu$A parallel to the layers.

The energy Landau-level fan diagram for a double quantum well consists of two sets of spin split LL separated by symmetric–antisymmetric energy gap. Figure 1 shows an experimental plot of the longitudinal resistance in the density–magnetic-field plane for a sample with the barrier thickness $d_b = 14$ Å. Such $n_s - B$ topological diagram, in general, corresponds to the energy LL fan diagram; however, several features are different. For example, in the level crossing regime, one may see, instead of the diamondlike structure, the so-called "ringlike" structure, which has been observed previously in double wells,[16] and square and parabolic wells with two occupied subbands.[17–19] These features, in principle, can be explained in terms of the nonmonotonic behavior of the Fermi energy at the Landau-level crossing point within the single-particle model.[18,19] The system is balanced at $n_s = 9 \times 10^{11} - 9.2 \times 10^{11}$ cm^{-2}. At the balance point and $B > 1$ T, the energy scale of the LL gaps is the following: the cyclotron gap $\hbar \omega_c$, where $\omega_c = eB/m$, m is the effective mass, is larger than all other energy gaps; the Zeeman energy $g \mu_B B$, where g is the effective Lande factor and μ_B is the Bohr magneton, is larger than the symmetric–antisymmetric gap because of the exchange-correlation effects; Δ_{SAS} is
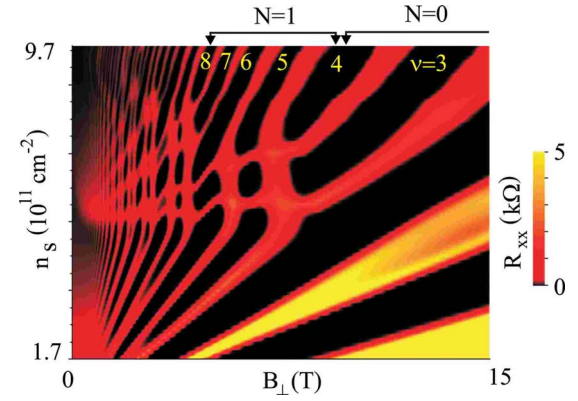

FIG. 1. (Color online) Experimental plot of the resistance in the density–magnetic-field plane for double-well structure with barrier thickness $d_b = 14$ Å for tilt angle $\Theta = 0$. Filling factors determined from Hall resistance are labeled. Filling factors $\nu = 4N+1$ and $\nu = 4N+3$ correspond to the tunneling gap.

smaller than the other energy gaps.[20] Therefore quantum Hall state minima at $\nu = 4N$ are related to the cyclotron gap, minima at $\nu = 4N+2$ correspond to Zeeman spitting, and minima at $\nu = 4N+1$ and $\nu = 4N+3$ correspond to Δ_{SAS} gaps.

Numerous scans were taken at various V_g, the magnetic field sweeps, for different tilt angles. Figures 2–4 show the resulting phase diagrams, or the plots of the longitudinal resistance R_{xx} in $B_\perp - B_\parallel$ plane for double wells with barrier thickness $d_b = 14$ Å, $d_b = 20$ Å, and $d_b = 31$ Å, consequently at the balance point. We recalculate $B_\perp = B \cos \Theta$ and $B_\parallel = B \sin \Theta$. The phase diagram clearly demonstrates that the minima in the resistance corresponding to the filling factors $\nu = 4N+1$ and $\nu = 4N+3$ vanish when the magnetic field is tilted. The vanishing of the resistance occurs in small range of in-plane field and is accompanied by vanishing of the Hall quantization. When the in-plane field increases, the energy gap at $\nu = 4N+1$ and $\nu = 4N+3$ vanishes and re-establishes several times for $N = 2, 3, 4, 5 \ldots$

From this map we measure the resistance at fixed filling factor or the value of the perpendicular magnetic field as a function of the in-plane field. Figure 5 shows the dependence
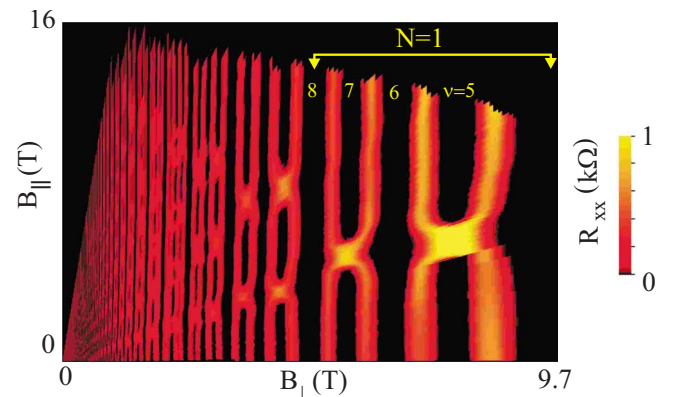

FIG. 2. (Color online) Experimental plot of the resistance in $B_\perp - B_\parallel$ plane for double-well structure with barrier thickness $d_b = 14$ Å. Filling factors determined from Hall resistance are labeled. Filling factors $\nu = 4N+1$ and $\nu = 4N+3$ correspond to the tunneling gap.
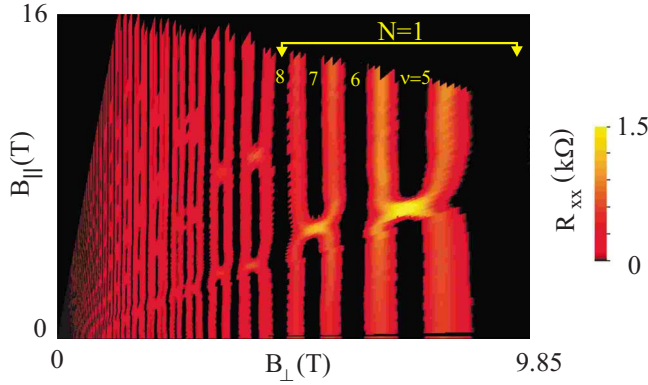
FIG. 3. (Color online) Experimentally determined plot of the resistance in $B_\perp - B_\parallel$ plane for double-well structure with barrier thickness d_b=20 Å.

of R_{xx} on parallel field for 14, 20, and 31 Å barrier samples. We may see almost periodical oscillations of the longitudinal resistance with the in-plane field with a periodicity proportional to the filling factor. Reentrance of the quantum Hall state at the filling factors $\nu=4N+1$ and $\nu=4N+3$ originates from the oscillations of the single-particle tunneling gap Δ_{SAS}. The resistance peak corresponds to the vanishing of the tunneling gap and the resistance minimum corresponds to the maximum of the tunneling amplitude. At these integer filling factors, R_{xx} exponentially depends on this energy gap $R_{xx} \sim R_0 \exp(-\Delta_{SAS}/2kT)$; therefore any decrease in the energy gap leads to an exponential growth in the resistance. In the tight-binding approximation it has been predicted that the tunneling amplitude is given by[10]

$$\Delta_{SAS} = \Delta_{SAS}^0 \exp\left(-\frac{Q^2 l_\perp^2}{4}\right) L_N^0\left(\frac{Q^2 l_\perp^2}{2}\right), \qquad (1)$$

where L_N^0 is a generalized Laguerre's polynomial, the wave vector Q is defined as $Q=d/l_\parallel^2$, where $l_\parallel = \sqrt{\hbar/eB_\parallel}$ is the magnetic length associated with the parallel magnetic field consequently. It is worth noting that in realistic samples, when the finite layer width is taken into account, d is the distance between maxima of the wave function [see Fig. 5(a)] and
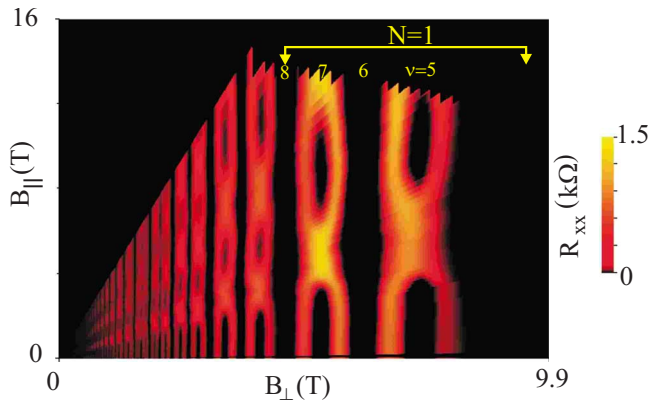

FIG. 4. (Color online) Experimentally determined plot of the resistance in $B_\perp - B_\parallel$ plane for double-well structure with barrier thickness d_b=31 Å.
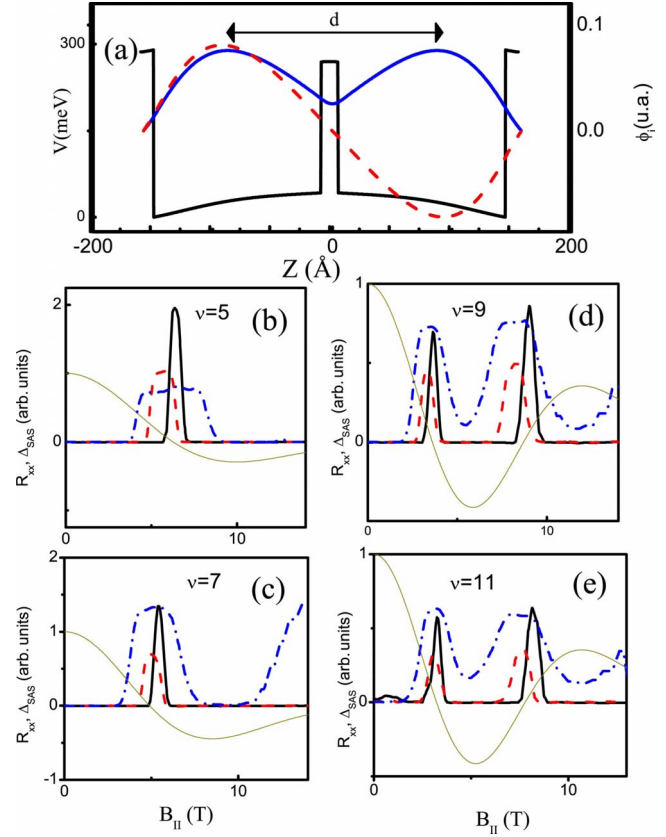

FIG. 5. (Color online) (a) Example of calculated wave functions in the DQW in the resonance point. [(b)–(e)] Dependence of R_{xx} at ν=5,7,9,11 on an in-plane magnetic field at T=50 mK for 14 (thick line), 20 (dash line), and 31 Å (dot-dash line) barrier bilayer structures. The thin solid lines show the variation in the tunneling amplitude Δ_{SAS} calculated from Eq. (1) with the parallel magnetic field for filling factors ν=5,7,9,11, corresponding to Landau levels [(a)and (b)] N=1 and [(c) and (d)] 2 for d=115 Å.

should be substituted by d_b+d_W. For N=1,2,3…, the tunneling amplitude is modulated by $B_\parallel$ and becomes negative in some range of the tilt angle (the energy per particle is simply proportional to the absolute value of the tunneling amplitude). The destruction of the tunneling gap in the presence of the in-plane field, however, has been reported in early studies of the quantum Hall bilayers.[20] Figure 5 shows the results of comparison of the data for three of our samples with different barrier widths and Eq. (1). Indeed it can be seen that the tunneling amplitude vanishes when the longitudinal resistance has a maximum. Note that the resistance maxima for barrier samples with d_b=20 Å and d_b=31 Å systematically occur at lower in-plane field in comparison with thinner barrier samples. From the comparison with theory, we deduce the distance d between maxima of the wave functions, indicated in the Table I. We may see that the value d_{exp} is 30%–40% smaller than the value expected for ideal bilayers. It is worth noting that the peak width in Fig. 5 strongly increases for wider barrier structure. This observation is consistent with our arguments that the resistance oscillates due to tunneling gap oscillations. The resistance in the quantum Hall minima can be described by thermally activation to broadened Landau levels; therefore for smaller
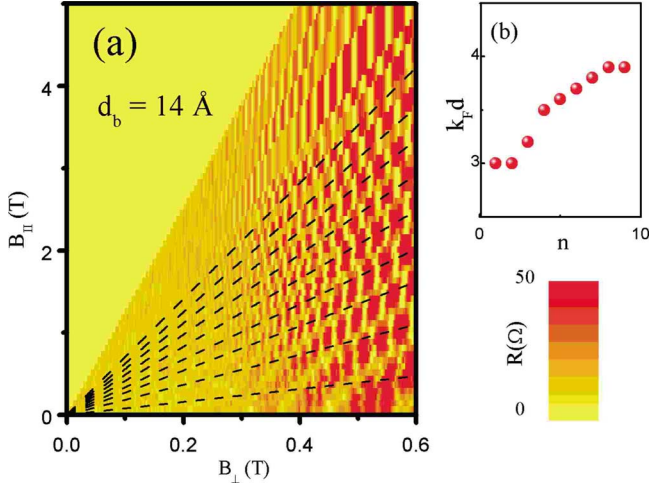
FIG. 6. (Color online) (a) Experimental plot of the resistance in the $B_\perp - B_\parallel$ plane for double-well structure with barrier thickness $d_b = 14$ Å. Dashed lines $B_\parallel / B_\perp = \tan \frac{\pi(n-1/4)}{k_F d}$, which pass through resistance maxima. (b) Parameter $k_F d$ deduced from the slopes of the lines.

tunneling gap, the resistance minimum is less pronounced and the peak is noticeably more broadened.

From the data in the presence of the in-plane magnetic field, we may conclude that the Landau fan diagram is strongly modified by the in-plane magnetic field. We observed this modification, for example, we found that the ring-like structures shift to the higher electron density, and the Landau-level crossing occurs at filling factors $\nu = 5$, 7, 9, and 11.

Now we focus on the results obtained at low perpendicular magnetic field. In this regime the Laguerre polynomials in Eq. (1) reduce to the Bessel function for the high Landau levels:

$$\Delta_{SAS} = \Delta_{SAS}^0 J_0\{k_F d \tan(\Theta)\}, \tag{2}$$

where J_0 is the Bessel function, $\tan(\Theta) = B_\parallel / B_\perp$.

At low magnetic field the magnetoresistance oscillations for two subbands are well described by the following expression:

$$\rho_{xx} \simeq \rho_0 \left\{ 1 - 4 e^{-\pi/\omega_c \tau_q} \mathcal{T} \cos\left(\frac{2\pi\varepsilon_F}{\hbar\omega_c}\right) \cos\left(\frac{\pi\Delta_{SAS}}{\hbar\omega_c}\right) \right\}, \tag{3}$$

where $\rho_0 = m/e^2 n\tau$ is the zero-field Drude resistivity, the Fermi energy ε_F is counted from the middle point between the subbands, the function $\mathcal{T} = (2\pi^2 T/\hbar\omega_c)/\sinh(2\pi^2 T/\hbar\omega_c)$ describes thermal suppression of the resistivity oscillations, τ is the transport scattering time, and τ_q is quantum lifetime. The expression (3) predicts beating of the SdH oscillations with Δ_{SAS} frequency. Equation (2) can be reduced by using the asymptotic behavior for the Bessel function $J_0(x) \sim \cos(x - \pi/4)/\sqrt{x}$. One can see that at $\Theta_n = \arctan\frac{\pi(n-1/4)}{k_F d}$, $\Delta_{SAS} = 0$ and SdH oscillation amplitude have a maximum value. Figure 6(a) shows experimental plot of the resistance in the $B_\perp - B_\parallel$ plane at low perpendicular magnetic field for double-well structure with barrier thickness
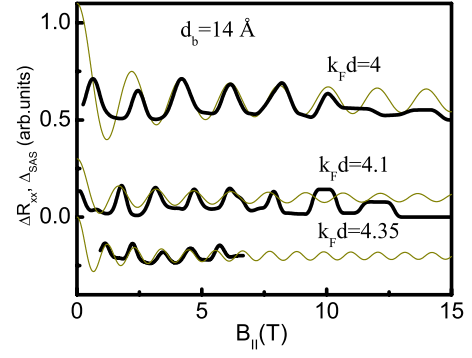

FIG. 7. (Color online) Resistance as a function of the in-plane magnetic field for $d_b = 14$ Å (thick lines) at $B_\perp = 1.25$ T, $B_\perp = 0.98$ T, and $B_\perp = 0.75$ T (from up to down). Curves are shifted for clarity. Thin lines Eq. (2).

$d_b = 14$ Å. We also plot the set of lines at certain angles $\tan \Theta = B_\parallel / B_\perp$ obtained from the magnetoresistance maxima. One can recognize the pattern of lines which coincides with this set of straight lines, especially for large index number n. We expect that the resistance maxima occurs at magic angles, when $\Delta_{SAS} = 0$. Therefore the slope of lines is determined by $\frac{\pi(n-1/4)}{k_F d}$, which allows the deduction of the parameter $k_F d$. Figure 6(b) demonstrates that this parameter depends on the value of the in-plane magnetic field. From this comparison we obtain the distance $d = 126 - 165$ Å, which agrees with the value extracted in the quantum Hall regime (see Table I). In perpendicular magnetic field at $\Theta = 0$, the resistance is described by SdH oscillations with beating and is determined by Eq. (3). Therefore the pattern of lines deviates from straight lines at small tilt angles, which is clearly seen in Fig. 6(a).

Finally we compare experimental results for magnetoresistance oscillations in low-field regime as a function of the in-plane field at fixed $B_\perp$ with Eq. (1). In Fig. 7 we show characteristic traces of resistance for $d_b = 14$ Å barrier sample. We have also performed a fitting of the tunneling gap oscillations [Eq. (2)] to the data with parameter $k_F d$ indicated in the figure. Using these parameters, we obtained the distance between wave-function maxima $d = 170 - 180$ Å for $d_b = 14$ Å barrier sample, which roughly agrees with the expected value (see Table I).

In the last part we reproduce the intuitive geometrical interpretation of the observed oscillatory effects as a manifestation of the Aharonov-Bohm effect in the titled magnetic field, first presented in Ref. 9. Figure 8(a) shows schematically two layers separated by the distance d in a tilted magnetic field. In the quasiclassical approximation, the electron motion in the presence of the perpendicular magnetic field $B_\perp$ is described by the cyclotron orbit with radius $R_c = \hbar k_F / e B_\perp$, where k_F is the Fermi wave vector.

Magnetic flux due to parallel component of the magnetic field $B_\parallel$ through the area $S = 2 R_c d$, as shown in Fig. 8(b), produces the phase shift between cyclotron orbits in different layers, which leads to the oscillations of the effective interlayer tunneling amplitude.[9] In momentum space in-plane magnetic field introduces the shift of the two Fermi surfaces $\Delta k_\parallel = e B_\parallel d / \hbar$ relative to each other,[20] as shown in Fig. 1(c).
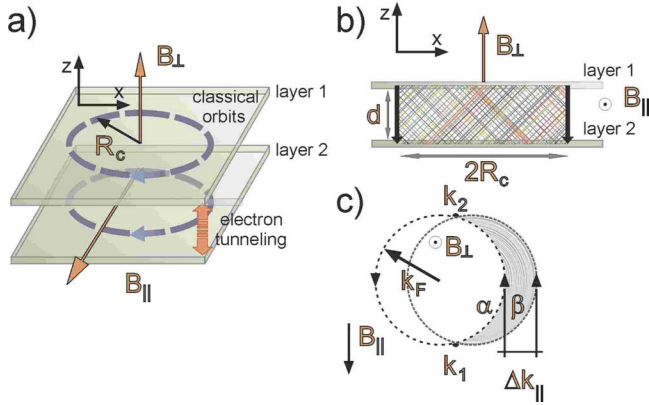
FIG. 8. (Color online) (a) Schematic of the bilayer system in the tilted magnetic field. Circles are cyclotron orbits. (b) Side view of the bilayers. Magnetic flux through the shaded area produces Aharonov-Bohm effect for the tunneling amplitude. (c) Fermi circles of the two-dimensional electron gas in bilayers in the presence of the parallel and perpendicular magnetic fields in momentum space. The Fermi circles are shifted by $\Delta k_{\parallel} = eB_{\parallel}d/\hbar$ relative to each other due to $B_{\parallel}$ component. Magnetic flux through the shaded area leads to the oscillations of the tunneling amplitude.

From energy and momentum conservation laws, it follows that the tunneling occurs at points k_1 and k_2. As in the real space, the interference of the trajectories α and β connecting the tunneling points should be taken into account for calculation of the interlayer tunneling amplitude. Magnetic flux due to perpendicular component of the magnetic field through the shaded area between trajectories α and β results in destructive or constructive interference at the opposite turning points. Indeed the Aharonov-Bohm effect in real [Fig. 8(b)] and momentum [Fig. 8(c)] spaces leads to the same tunneling amplitude oscillations with the tilt angle.

From the above discussions, we conclude that our experimental observation of the oscillations of the tunneling gap is consistent with predictions[9,10] given by Eqs. (1) and (2), and results from the interlayer Aharonov-Bohm oscillations as it was recognized first in Ref. 9. We may see from Fig. 5 that the peak /valley ratio of the magnetoresistance oscillations can be larger than 10^4, which is the strongest periodical resistance modulation by magnetic field due to interference effect.

III. CONCLUSION

In conclusion, we have studied the parallel magnetotransport in bilayer electron systems in the tilted magnetic field in the quantum Hall effect and SdH oscillation regimes. We have found striking similarity between the magnetoresistance oscillations in our system and the angular magnetoresistance oscillations in many other layered materials such as organic conductors based on BEDT-TTF and its derivatives,[21] intercalated graphite,[22] $Tl_2B_2CuO_6$,[23] and quasi-one-dimensional organic semiconductors.[8] Note that, in contrast to the longitudinal resistance in bilayer systems, AMROs have been observed in the interlayer resistivity ρ_z. We attribute angular magnetoresistance oscillations in parallel transport in bilayer system to the interlayer Aharonov-Bohm effect, and therefore, the oscillations in bilayers have the same origin, as AMRO in other layered quasi-two-dimensional and quasi-one-dimensional systems.

[1] Y. Imry and R. A. Webb, Sci. Am. **260**, 56 (1989).

[2] R. A. Webb, S. Washburn, C. P. Umbach, and R. B. Laibowitz, Phys. Rev. Lett. **54**, 2696 (1985).

[3] G. Timp, A. M. Chang, J. E. Cunningham, T. Y. Chang, P. Mankiewich, R. Behringer, and R. E. Howard, Phys. Rev. Lett. **58**, 2814 (1987).

[4] K. Ismail, S. Washburn, and K. Y. Lee, Appl. Phys. Lett. **59**, 1998 (1991).

[5] M. Casse, Z. D. Kvon, G. M. Gusev, E. B. Olshanetskii, L. V. Litvin, A. V. Plotnikov, D. K. Maude, and J. C. Portal, Phys. Rev. B **62**, 2624 (2000).

[6] A. Bachtold, C. Strunk, J.-P. Salvetat, J.-M. Bonard, L. Forró, T. Nussbaumer, and C. Schönenberger, Nature (London) **397**, 673 (1999).

[7] N. A. J. M. Kleemans, I. M. A. Bominaar-Silkens, V. M. Fomin, V. N. Gladilin, D. Granados, A. G. Taboada, J. M. García, P. Offermans, U. Zeitler, P. C. M. Christianen, J. C. Maan, J. T. Devreese, and P. M. Koenraad, Phys. Rev. Lett. **99**, 146808 (2007).

[8] B. K. Cooper and V. M. Yakovenko, Phys. Rev. Lett. **96**, 037001

(2006).

[9] V. M. Yakovenko and B. K. Cooper, Physica E (Amsterdam) **34**, 128 (2006).

[10] J. Hu and A. H. MacDonald, Phys. Rev. B **46**, 12554 (1992).

[11] G. M. Gusev, A. K. Bakarov, T. E. Lamas, and J. C. Portal, Phys. Rev. Lett. **99**, 126804 (2007).

[12] P. Moses and R. H. McKenzie, Phys. Rev. B **60**, 7998 (1999).

[13] N. C. Mamani, G. M. Gusev, T. E. Lamas, A. K. Bakarov, and O. E. Raichev, Phys. Rev. B **77**, 205327 (2008).

[14] A. Palevski, F. Beltram, F. Capasso, L. Pfeiffer, and K. W. West, Phys. Rev. Lett. **65**, 1929 (1990).

[15] E. Zaremba, Phys. Rev. B **45**, 14143 (1992).

[16] A. G. Davies, C. H. W. Barnes, K. R. Zolleis, J. T. Nicholls, M. Y. Simmons, and D. A. Ritchie, Phys. Rev. B **54**, R17331 (1996).

[17] X. C. Zhang, D. R. Faulhaber, and H. W. Jiang, Phys. Rev. Lett. **95**, 216801 (2005).

[18] C. Ellenberger, B. Simovič, R. Letureq, T. Ihn, S. E. Ulloa, K. Ensslin, D. C. Driscoll, and A. C. Gossard, Phys. Rev. B **74**, 195313 (2006).

[19] C. A. Duarte, G. M. Gusev, A. A. Quivy, T. E. Lamas, A. K. Bakarov, and J. C. Portal, Phys. Rev. B **76**, 075346 (2007).

[20] G. S. Boebinger, A. Passner, L. N. Pfeiffer, and K. W. West, Phys. Rev. B **43**, 12673 (1991).

[21] K. Kajita, Y. Nishio, T. Takahashi, R. Kato, H. Kobayashi, W. Sasaki, A. Kobayashi, and Y. Iye, Solid State Commun. **70**, 1189 (1989).

[22] Y. Iye, M. Baxendale, and V. Z. Mordkovich, J. Phys. Soc. Jpn. **63**, 1643 (1994).

[23] N. E. Hussey, M. Abdel-Jawad, A. Carrington, A. P. Mackenzie, and L. Ballcas, Nature (London) **425**, 814 (2003).